LA-UR--92-3

DE92 007428

A-UR- 92-0003

Los Alamos National Laboratory is operated by the University of California for the United States Department of Energy under contract W-7405-ENG-36

TITLE: NUMERICAL SIMULATION OF TWO-DIMENSIONAL SINGLE- AND MULTIPLE-MATERIAL FLOW FIELDS

AUTHOR(S): Amalia R. Lopez, Roy S. Baty, SNL
Bryan A. Kashiwa, T-3

SUBMITTED TO: 1992 ASME Cavitation and Multiphase Flow Forum, Los Angeles, California, June 22--25, 1992

Los Alamos National Laboratory
Los Alamos, New Mexico 87545

DISCLAIMER

Numerical Simulation of Two-Dimensional Single- and Multi-Material Flow Fields

Amalia R. Lopez, Roy S. Baty
Aerospace Technology Department
Sandia National Laboratories
Albuquerque, NM 87185
and
Bryan A. Kashiwa
Theoretical Division
Los Alamos National Laboratory
Los Alamos, NM 87545

INTRODUCTION

Over the last several years, Sandia National Laboratories has had an interest in developing capabilities to predict the flow fields around vehicles entering or exiting the water at a wide range of speeds. Such prediction schemes have numerous engineering applications in the design of weapon systems. For example, such a scheme could be used to predict the forces and moments experienced by an air-launched anti-submarine weapon on water-entry. Furthermore, a water-exit prediction capability could be used to model the complicated surface closure jet resulting from a missile being shot out of the water.

The CCICE[1,2] (Cell-Centered Implicit Continuous-fluid Eulerian) code developed at Los Alamos National Laboratory (LANL) was chosen to provide the fluid dynamics solver for high speed water-entry and water-exit problems. This implicit time-marching, two-dimensional, conservative, finite-volume code solves the multi-material, compressible, inviscid fluid dynamics equations. The incompressible version of the CCICE code, CCMAC[3] (Cell-Centered Marker and Cell), was chosen for low speed water-entry and water-exit problems in order to reduce the computational expense.

These codes were chosen to take advantage of certain advances in numerical methods for computational fluid dynamics (CFD) that have taken place at LANL. Notable among these advances is the ability to perform implicit, multi-material, compressible flow simulations, with a fully cell-centered data structure. This means that a single set of control volumes are used, on which a discrete form of the conservation laws is satisfied. This is in contrast to the more classical staggered mesh methods, in which separate control volumes are defined for mass and momentum.

This new class of computational schemes has enabled Los Alamos to develop a library of hydrocodes, each of which uses the same cell-centered data structure. The library of codes is referred to as CFDLIB[4] and now contains a full set of hydrocodes for high-speed, all speed, and incompressible flow. Additional volumes exist for multiphase flow in each of the flow speed regimes.

The LANL hydrodynamics codes were designed originally to be applied to high explosive problems with very violent physics and extremely short time scales. The current version of these codes have never been benchmarked extensively for the flow regimes encountered in the water-entry and water-exit problems of interest. Therefore, this report presents the results of a set of numerical experiments performed to benchmark CCICE and CCMAC, and to determine their limitations as flow solvers for water-entry and water-exit simulations.

HYDRODYNAMICS CODES

The LANL hydrodynamics codes currently used by at Sandia are CCICE, and CCMAC. These codes are all related by a common set of features. Some of the features shared by these codes include: finite-volume computational schemes with cell-centered state variables, multi-block data structure for efficient processing on modern supercomputers, and an ALE (Arbitrary-Lagrangian-Eulerian) computational cycle. The ALE technique is one of the most important features of these codes because it prevents mesh tangling by splitting the hydrodynamic time-step into a Lagrangian phase and a rezone-remap phase. Details on this approach are described by Addessio et al.[1] Another important feature common to these codes is the use of cell-centered state variables. In particular, the use of cell-centered velocities provides an efficient description of the interface between cells and a consistent method to maintain the conservation of mass and energy throughout the computation of a multi-material problem.

The computational domain for CCICE and CCMAC assumes a set of multiple, interacting cells, each of which contains a single material with a single velocity vector. The motion of an inviscid fluid in these cells is governed by the equation, describing conservation of mass and momentum

$$\frac{d}{dt}\int_{V(t)} \rho dV + \int_{S(t)} \rho(\hat{u} - \hat{u}_a)\cdot \hat{A} dS = 0 \qquad (1)$$

$$\frac{d}{dt}\int_{V(t)} \rho \hat{u} dV + \int_{S(t)} \rho \hat{u}(\hat{u} - \hat{u}_a)\cdot \hat{A} dV = -\int_{S(t)} p\hat{A} dS + \int_{V(t)} \rho \hat{f} dV \qquad (2)$$

where, ρ is the density, p is the pressure, $\hat{u}$ is the fluid velocity, $\hat{u}_a$ is the control volume velocity, and f is the body force. $V(t)$ and $S(t)$ represent the control volume and its surface area, respectively. For the compressible problems the above equations are augmented with the energy equation and equations of state. Further details about the equations used to model the fluid mechanics are described by Addessio et al.[1] and Thompson[5].

The control volume velocity $\hat{u}_a$ has two important limiting values. In the first case $\hat{u} = \hat{u}_a$, or equivalently, the control volume is allowed to move with the fluid. This gives a Lagrangian description of the fluid motion. In the second case $\hat{u}_a = 0$, which is the Eulerian description of fluid motion. The hydrodynamics codes use the ALE approach which is a combination of the fluid dynamics (a Lagrangian phase) and a coordinate transformation due to the mesh motion (a remapping phase).

In the remapping phase, these codes have two discretization options. The first option is called the van Leer advection operator, which discretizes the

equations directly without knowledge of the material interface. The second option is called the mixed-cell[5] approach and assumes knowledge of a material interface. The second option is used only at material interfaces and the first option is used everywhere else.

CCICE was written by LANL to investigate various numerical methods that could calculate multi-material dynamics with strong distortions and slip between and within fluids in two and three dimensions. The ICE method was developed by Harlow and Amsden[6] to give a numerically stable and efficient means for calculating two-dimensional, transient, viscous fluid flows for Mach numbers from zero to infinity. The central feature of the ICE technique is the solution of an auxiliary equation for an estimate of the time-advanced pressure. This pressure is then used to compute the pressure force term in the momentum equations. The present version of CCICE solves the equations of motion for a two-dimensional, compressible, unsteady, inviscid, multi-material fluid with an implicit, cell-centered, time-marching numerical technique. In addition to the viscosity, the body forces, the heat-flux and the energy-release terms are not modeled in the current version of CCICE. The convergence parameter used in this method is for the pressure field. Since the present code provides a robust numerical method to solve complicated single-phase flows, it has shown a great deal of potential for simulating accurately high speed water-entry and water-exit problems.

For low speed water-entry and water-exit problems, CCMAC the incompressible version of CCICE is used. The incompressible scheme employed in CCMAC is the ICE method in the limit of zero Mach number. By solving an incompressible system instead of a compressible system, the computational time is reduced for low speed problems. CCMAC solves the equations for a two-dimensional, unsteady, inviscid, multi-material fluid dynamics with an implicit time-marching numerical technique. The heat-flux and energy terms are again not included in the equations, however, CCMAC does include the gravity term. The CCMAC technique iteratively solves this single system of inviscid equations. In addition, a surface pressure integrator was added to compute the unsteady forces and moments experienced by a body during water-entry or water-exit. The pressure integrator has also been coupled with an algorithm to compute the rigid body motion. These new capabilities could also be applied to CCICE. This modification is possible because the hydrodynamics codes are written modular form, making specialized development relatively simple.

Within the CFDLIB codes, there are several boundary condition options: (1) reflective or symmetry, (2) specified pressure, (3) outflow or zero gradient, (4) inflow, (5) boundary between blocks, (6) curved, rigid, free-slip, and (7) specified velocity. Both the reflective and curved, rigid, free-slip boundary conditions specify a zero normal-velocity component and a tangential velocity component which is the same as the tangential-component of the adjacent cell-centered velocity.

The hydrodynamics codes CCICE and CCMAC were designed as general purpose, but have been applied and verified mainly for explosive problems with very small time scales. For these types of problems, the effect of gravitation is negligible and gravity was not modeled prior to the current interest in water-entry and water-exit problems. Several numerical experiments were performed to test the codes for non-explosive fluid mechanics problems with and without buoyancy.

Computer times for all of the numerical experiments in this paper ranged from 1 to 30 minutes on a CRAY Y/MP. CCMAC solutions were generally 3 times faster than the CCICE solutions. For complex shapes or multi-material problems where the grid becomes distorted, computational times can increase to on the order of an hour.

NUMERICAL EXPERIMENTS

This section presents the fluid mechanics problems that were run to benchmark CCICE and CCMAC. Two simple incompressible, single material, steady problems were chosen to determine how to define the boundary conditions, convergence criteria, and stability parameters in both codes. Once the steady problems were completed, two multi material, unsteady problems were run to check the gravity model and the rigid body dynamics solver built into CCMAC. The results of these numerical experiments were compared, when possible, to the other analytical, experimental, or other numerical results.

Two-Dimensional Airfoil Calculation

This numerical experiment computes the steady flow of air around a circular-arc on an infinite flat plate. This geometry was used to approximate a circular-arc airfoil in uniform flow at zero angle of attack. This particular example was studied to understand which boundary conditions would yield an accurate solution.

The circular-arc airfoil is defined as the image of a circle under the action of a Joukowski transformation. This transformation is a conformal mapping of regions of the complex plane into itself. The Joukowski map[7] is defined by:

$$\zeta = z + \frac{C^2}{z} \qquad (3)$$

where C is a real number, and z and ζ are complex variables. The values for C and the domain of Equation 3 were chosen so that the length of the arc airfoil is eight times its height above the flat plate.

The mesh and the steady pressure field surrounding the circular-arc, flat plate are shown in Fig. 1. In this figure, the different pressure levels are depicted by different contour shades. The present results are for CCICE, similar results were obtained using CCMAC. The mesh shown in Fig. 1 is an algebraic grid with 20x91 grid points.

For this problem, a free-slip boundary condition was used along the entire left side of the domain where the circular-arc on a flat plate is located. On the right side of the domain, the CCICE calculation used a reflective boundary condition, while the CCMAC calculation used an outflow boundary condition. Both codes used an inflow boundary condition along the bottom side of the domain and an outflow boundary condition along the top of the domain. The inflow boundary condition was set so that air flowed into the domain at a temperature of 340 K, a density of 1 kg/m^3, and a velocity of 15 m/s in the +Y direction. In addition to boundary conditions, initial conditions were specified in the domain using the same values as at the inflow boundary.

In Fig. 1, the pressure increases as the flow approaches the leading edge of the arc. It then decreases along the arc as the flow accelerates to the arc's mid-point. Finally, the pressure increases as the flow compresses towards the trailing edge of the arc. This pressure distribution is nearly symmetrical, which indicates that the solution approximates qualitatively an inviscid, irrotational solution.

The results computed with CCICE and CCMAC can be compared with the potential flow solution for a circular-arc airfoil because the analytical solution provides a good approximation to the present problem. The potential flow solution for the flow over a circular-arc airfoil may be constructed using elementary complex analysis. This solution is well known and described by Kuramcheu[8].

Fig. 2 shows the comparison between the numerical results and the analytic solution. It should be noted that the numerical results represent the cell-centered values, while the analytic result is located on the surface.

This figure shows that CCICE and CCMAC results agree well with the exact solution. The maximum error between the numerical and analytic results is on the order of 10^{-1}. The difference between the two numerical results is partially due to the different boundary conditions used along the right side of the domain. Specifying a reflective or symmetry boundary implies a mirrored surface is located equidistant to the right. Therefore, the physical interpretation of the flow field is of flow between two arcs. Since the flow is incompressible, the fluid will have to speed up as it enters the reduced cross-section and lower its pressure. Conversely, CCICE used an outflow boundary condition which also specifies a zero pressure gradient but allows mass flow out of the domain. Therefore, the fluid is not artificially accelerated in the CCICE calculation and its pressure will be lower than the CCMAC result. Another reason for this difference in results is that the codes used different convergence methodologies. Since the flow is essentially incompressible, small changes in the convergence criteria for CCICE can have a relatively large effect.

The CCICE solution also has numerical oscillations near the leading and trailing edges of the circular arc. In most cases, numerical oscillations can be removed by refining the grid. However, the fact that both numerical calculations were performed on the same grid indicates that possibly the difference in the convergence methodologies between CCICE and CCMAC may have caused the oscillations in the CCICE solution.

Axisymmetric Cone-Cylinder-Boattail Calculation

The next example computes the steady flow of air around a cone-cylinder

boattail. In this example, the cone half angle is 14.04 degrees, and the boattail angle is 6.0 degrees.

The mesh and the steady pressure field surrounding the cone-cylinder-boattail are shown in Fig. 3. The pressure contour results in this figure are for CCICE; similar results were obtained using CCMAC. The mesh shown in Fig. 3 is an algebraic grid with 61x131 grid points.

For this problem, a reflective boundary condition was specified along the axis of symmetry. The body was defined using a free-slip boundary. Again, the boundary condition selected for the right side of the domain was based on the code: reflective for CCICE and outflow for CCMAC. The inflow boundary condition was set so that air flowed into the domain at a temperature of 278 K, a density of 1 kg/m^3, and a velocity of 50 m/s in the +Y direction, while, an outflow boundary was specified along the top of the domain. The initial conditions were again set equal to the values used at the inflow boundary.

The numerical solutions were compared to a potential flow solution computed with SANDRAG[9]. This potential flow code has been benchmarked against experimental data and gives very good agreement for cone-cylinder-boattails with slender geometries for Mach numbers up to 0.5 in air.

Fig. 4 shows the numerical results of CCICE, CCMAC and SANDRAG. In this figure, CCICE and CCMAC both give results which are in excellent agreement with SANDRAG. It should be noted that the CCICE and CCMAC results represent cell-centered values, while the SANDRAG solution represents the pressure on the surface of the body. The numerical oscillations in the SANDRAG solution at the start of the conical section are a result of the slender body assumption in the code which starts to break down for large cone angles. The numerical oscillations in the CCICE and CCMAC solutions at the start of the cylindrical section are attributed to the growth of a second order instability in the advection algorithm.

One important point to note about the CCICE solution is that it predicts the pressure drops on the cone-cylinder-boattail. These dips are the result of discontinuities in the curvature of the body. Any code used to model cavitating flow must capture this behavior accurately. This suggests that CCICE could be used to model the unsteady pressure field in a cavitating flow field.

Rayleigh-Taylor Calculation

The last two problems in this report test the multi-material, gravity and rigid body dynamics prediction capabilities of the CCMAC code. The first of these problems is presented in this section and simulates the initial growth of a Rayleigh-Taylor instability. This instability occurs when a heavy fluid is placed over a light fluid and gravity causes the fluids to invert. A Rayleigh-Taylor problem was chosen to check the multi-material and gravity models in the code.

The Rayleigh-Taylor problem simulated the experiment of Ratafia[10] in which water was initially above alcohol and the interface between the two fluids was perturbed with a sine wave of shallow amplitude. The initial conditions specified water at a density of 1000 kg/m^3 and alcohol at a density of 820 kg/m^3 with zero velocity.

The solution computed with CCMAC for the initial stages of the Rayleigh-Taylor instability are compared with the analytical results predicted from linearized potential flow theory. Using this theory, the interface η between two fluids, perturbed with a sine wave, has the following functional form:

$$\eta = \varepsilon \exp\left(\frac{2\pi}{\lambda}\sigma t\right) \cos\left(\frac{2\pi}{\lambda}x\right) \qquad (4)$$

where ε is the amplitude and λ is the wavelength of the sine curve. Here the quantity, σ, is an eigenvalue describing the temporal growth or decay of the interface disturbance as a function of the two densities. For the Rayleigh-Taylor problem, the eigenvalue reduces to:

$$\sigma = \sqrt{\frac{g}{2\pi}\frac{\rho_w - \rho_a}{\rho_w + \rho_a}} \qquad (5)$$

where ρ_w and ρ_a are the densities of water and alcohol respectively. Periodic boundary conditions are assumed in the theory. Further details about these equations may be found in Currie[11].

Figs. 5a-c show the comparison of the interface predicted with CCMAC to that given by linear theory. These results suggest that this code does a good job of approximating the Rayleigh-Taylor instability for the first 0.4 seconds. The figures also shows that the numerical results are slower than the analytical solution. This difference may be due to the use of free-slip boundary conditions in the numerical simulation.

Figs. 6a-c show CCMAC density contours at later points in time. In order to benchmark the results of CCMAC for the Rayleigh-Taylor instability outside the range of linear theory, the numerical results were compared with experimental results. This comparison suggests that the numerical results correctly describe the qualitative features of this mixing problem. Again, the numerical results were slower than the experimental observations. This difference may be attributed to modeling the experiment with a two-dimensional code. Also, fluid viscosity and surface tension are not modeled in CCMAC and may have prevented the breakdown of the cap region shown in Fig. 6c.

Incompressible Sphere Water-Entry Calculation

This section presents the final problem that was analyzed for this report: a simulation of the unsteady flow field around an axisymmetric rigid body entering water at a zero angle of attack. For this simulation, a sphere of diameter 0.025 m entered the water and the resulting impact acceleration experienced by the sphere was computed. This example was run to demonstrate that realistic low speed water-entry problems could be simulated with CCMAC.

Fig. 7 shows the grid block structure and boundary conditions for the sphere. The computational domain was divided into five blocks with the dimensions as indicated in the figure. Here, the water surface is represented by the dotted line crossing blocks 1 and 2. A five block structure was used in order to generate a quality grid around the sphere. Since the left side of the domain is along the axis of symmetry, a reflective boundary was specified. The body, which is along the top of block 1, the left side of block 3, and the bottom of block 4, was defined using the specified velocity boundary condition. The bottom, top, and right sides of the domain were all specified as outflow boundaries since this simulation was performed with CCMAC. The initial conditions were used to specify water at a density of 1000 kg/m^3 and air at a density of 1 kg/m^3 with zero velocity.

Two water-entry simulations were run for this example. These simulations included two air-water interface models. For each of these simulations, the motion of the sphere was started impulsively with a specified velocity from a fixed height of 0.023 m above the water interface. In addition, the use of the rigid body dynamics option required that the mass of the sphere, 0.665 kg, and a moment of inertia, 4.1563E-05 kg•cm^2, be specified for this problem.

In addition to solving the fluid dynamic equations describing an incompressible fluid, CCMAC has been modified to solve the two-dimensional equations of motion for a rigid body:

$$\sum \hat{F} = m\hat{a} \qquad (6)$$

$$\sum \hat{M} = \frac{d\hat{H}}{dt} \qquad (7)$$

Equations (6) and (7) are expressed in an inertial coordinate system fixed relative to the water surface. The origin of this system is shown in Fig. 7. Moreover, the reference point (●) for these equations is also shown, in this figure. The linear acceleration predicted by these equations for the sphere is the result of the fluid structure interaction. At the end of each time step in the calculation of the fluid motion, CCMAC uses the predicted pressure field to solve the rigid body equations and update the position of the sphere. Furthermore, the total acceleration is used to estimate the sphere impact loads on water entry. This acceleration is defined by:

$$a = \sqrt{a_z^2 + a_y^2} \qquad (8)$$

where the Z direction is coincident with the water surface, while the Y direction is perpendicular to the water surface. The non dimensional acceleration shown in Fig. 8 is the linear acceleration divided by gravity, 9.8 m/s.

Two distinct interface models were used to describe the air-water transition region. The first interface model was a mass transport model that smeared out the interface over a few cells. This interface model did not produce good results when this transition region had a length scale on the order of a fourth

of the radius of the sphere. However, as the grid was refined, the interface region was physically smaller which tended to produce better results. The second interface model used the mixed-cell capability of the CCMAC code. This model captured more of the discontinuous nature of the air-water interface and provided more realistic numerical results.

In order to benchmark the results, the water-entry impact accelerations predicted for the sphere with CCMAC were compared against the theoretical work of Shiffman and Spencer, and the experimental work of Moghisi and Squire outlined in Ref. 12. Fig. 8 shows the predicted impact acceleration for the two air-water interface models, assuming a constant entry velocity of 2.43 m/s, against the theoretical and the experimental results. Both the theoretical and experimental acceleration values were obtained from the quoted drag coefficient values by scaling these values with the cross-sectional area of the sphere, the mass of the sphere, and the dynamic pressure based on the density of water and the velocity of the sphere. This figure shows that the sphere had a small amount of deceleration, 0.01, in the air before it impacted the water surface. In addition, the solution obtained using the mass transport option shows the sphere impacting the interface at a non-dimensional depth of -0.075. Since the air-water interface is located at exactly zero on the b-axis, this distance is an indication of the amount of interface smear produced by this model. The solution obtained using the mixed-cell model shows the sphere impacting the interface at a non-dimensional depth of -0.01. This slight difference in distance from the real interface is not due to interface smear but to the cell-centered structure of the code. Although the mixed-cell model described the impact acceleration more accurately, numerical oscillations did occur in this solution. These oscillations are numerical artifacts that emerge because of the second order treatment in the advection operator. Overall, CCMAC predictions generate an accurate approximation of the sphere's initial water-entry acceleration.

CONCLUSIONS

This report has presented the results of a set of numerical experiments performed to benchmark the LANL hydrodynamics codes, CCICE and CCMAC, and to determine their limitations as flow solvers for water-entry and water-exit problems. The steady problems were designed to determine the boundary conditions, convergence criteria, and stability parameters needed for these codes to yield realistic solutions. Once the steady flow problems were understood for CCICE and CCMAC, unsteady problems were run with CCMAC to test the gravity, multi-material and rigid body dynamics subroutines.

The results of these numerical experiments suggest that CCICE and CCMAC may be applied to simulate accurately a large variety of steady and unsteady two-dimensional flow problems. For the steady flow problems, both codes produced results which were in excellent agreement with the accepted inviscid solutions. Moreover, for the unsteady problems, CCMAC produced results which were in very good agreement with experimental data.

ACKNOWLEDGMENT

The authors wish to thank Timothy J. Bartel of the Thermophysics Division of Sandia National Laboratories for his helpful advice on applying these codes. This work was performed at Sandia National Laboratories for the U.S. Department of Energy under contract number DE-AC04-76DP00789.

REFERENCES

1. Harlow, F. H., and Amsden, A. A., 1971, "A Numerical Fluid Dynamics Calculation Method for All Flow Speeds," *Journal of Computational Physics*, Vol. 8, pp. 197-213.
2. Hirt, C. W., and Amsden, A. A., 1974, and Cook, J. L., "An Arbitrary Lagrangian-Eulerian Computing Method for All Flow Speeds," *Journal of Computational Physics*, Vol. 14, pp. 227-253.
3. Addessio, F. L., et al., 1990, "CAVEAT: A Computer Code for Fluid Dynamics Problems with Large Distortion and Internal Slip," LA-10613-MS-REVISED, Los Alamos National Laboratory, Los Alamos, NM.
4. Baumgardner, J. R., et al., 1990, "CFDLIB: A Library of Computer Codes for Problems in Computational Fluid Dynamics," LA-UR90-1361, Los Alamos National Laboratory, Los Alamos, NM.
5. Thompson, P. A., 1972, Compressible-Fluid Dynamics, McGraw-Hill, Inc., New York, pp. 41-49.
6. Johnson, N. L., et al., to appear, "CAVEAT: Current Extensions and Future Capabilities," Los Alamos National Laboratory Report.
7. Harlow, F. H., and Amsden, A. A., 1968, "Numerical Calculation of Almost Incompressible Flow," *Journal of Computational Physics*, Vol. 3, pp. 80-93.
8. Karamcheti, K., 1966, Principles of Ideal-Fluid Aerodynamics, John Wiley & Sons, New York, pp. 479-484.
9. Wolfe, W. P., and Oberkampf, W. L., 1985, "SANDRAG: A Computer Code for Predicting Drag of Bodies of Revolution at Zero Angle of Attack in Incompressible Flow," SAND85-0515, Sandia National Laboratories, Albuquerque, NM.
10. Ratafia, M., 1973, "Experimental Investigation of Rayleigh-Taylor Instability," *Physics of Fluids*, Vol. 16, pp. 1207-1210.
11. Currie, I. G., 1974, Fundamental Mechanics of Fluids, McGraw-Hill, Inc., New York, pp. 209-214.
12. Moghisi, M., and Squire, P. T., 1981, "An Experimental Investigation of the Initial Force of Impact on a Sphere Striking a Liquid Surface," *Journal of Fluid Mechanics*, Vol. 108, pp. 133-146.

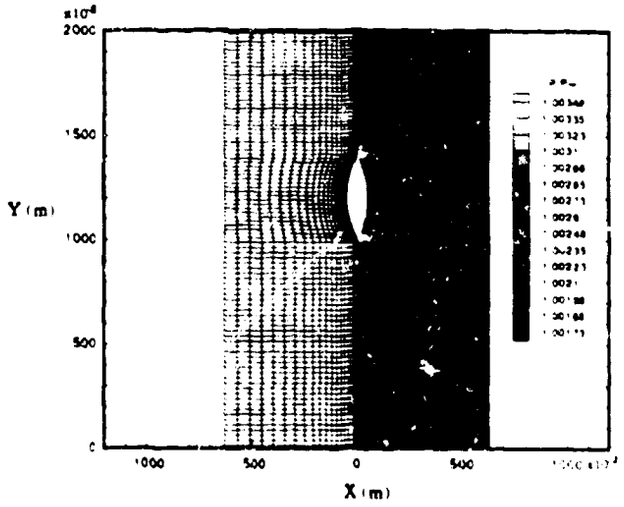

Figure 1: A typical mesh reflected against steady pressure contours for the circular-arc on an infinite flat plate.

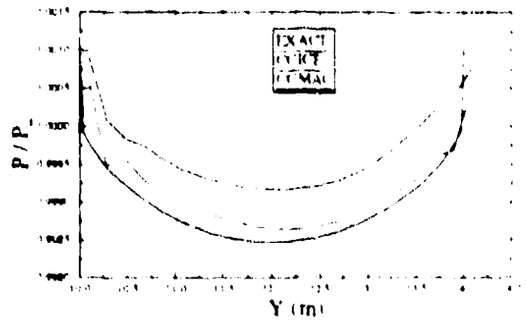

Figure 2: Surface pressure comparisons of the analytic solution for the circular-arc, flat plate with the numerical solutions of CCICE and CCMAC.

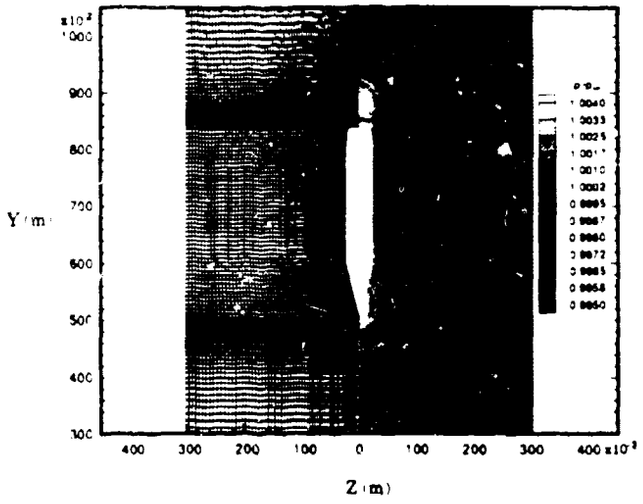

Figure 3 A typical mesh reflected against steady pressure contours for the cone-cylinder-boattail

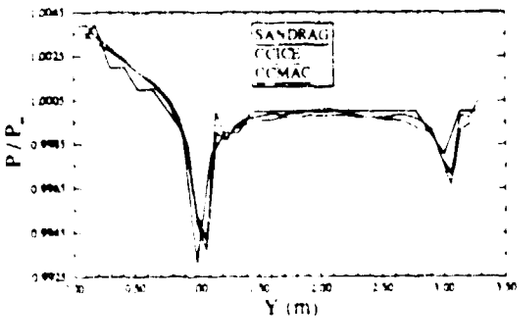

Figure 4: The pressure distribution along the surface of the cone-cylinder boattail computed using SANDRAG, CCICE, and CCMAC

Figures 6a-c: The development of the Rayleigh-Taylor instability for three points in time

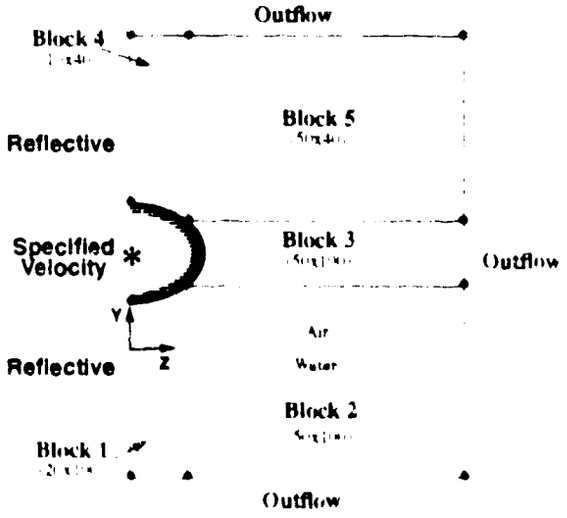

Figure 7: The grid block structure and boundary conditions for the sphere water impact problem (figure not to scale)

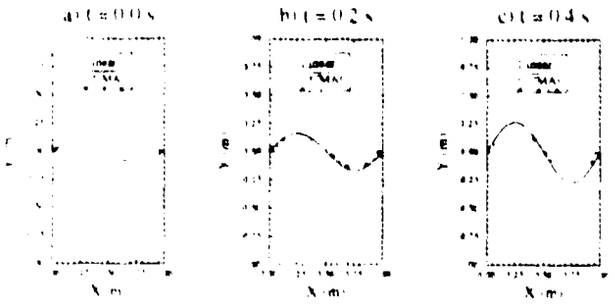

Figures 5a-c: These figures compare the interface predicted from linear theory with the results computed using CCMAC in the first 0.4 seconds

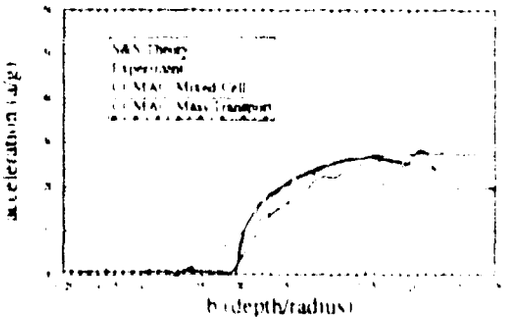

Figure 8: Acceleration plot comparing the two air water interface models at a velocity of 2.43m/s with the theoretical results of Shiffman and Spencer and the measurements of Mughal and Squire